Electrospray Characteristic Curves: In Pursuit of Improved Performance in the Nanoflow Regime

ARTICLE *in* ANALYTICAL CHEMISTRY · DECEMBER 2007

Impact Factor: 5.64 · DOI: 10.1021/ac0707986 · Source: PubMed

Published in final edited form as:
Anal Chem. 2007 November 1; 79(21): 8030–8036. doi:10.1021/ac0707986.

Electrospray characteristic curves: in pursuit of improved performance in the nano-flow regime

Ioan Marginean, **Ryan T. Kelly**, **Jason S. Page**, **Keqi Tang**, and **Richard D. Smith**
Biological Sciences Division, Pacific Northwest National Laboratory, P.O. Box 999, Richland, Washington 99352

Abstract

Depending on its coordinates in the parameter space, an electrospray can manifest in one of several known regimes – stable, quasi-stable, transitional-chaotic, and non-axial – that ultimately impact measurement sensitivity and precision. An electrospray operating in cone-jet regime provides large and stable spray current, as well as smaller initial droplets that are prerequisites for higher sensitivity and quality mass spectrometric analyses. However, the dynamic conditions encountered in gradient elution-based liquid separations create difficulties for continuous operation in this regime throughout the analysis. We present a preliminary study aimed at stabilizing the electrospray in the cone-jet regime. On the basis of spray current measurements obtained using solvent conditions typically found in liquid chromatography-mass spectrometry, an improved description of the cone-jet stability island is provided by including transitions to and from the recently described astable regime. Additionally, the experimental conditions in which the astable regime marks the transition between pulsating and cone-jet regimes are further clarified.

Keywords

Electrospray characteristic curves; electrospray regimes; cone-jet mode; spray current measurements

INTRODUCTION

The introduction of soft ionization methods[1-3] enabled mass spectrometric analysis of large biopolymers, including the use of electrospray ionization (ESI) to couple liquid chromatography (LC) to mass spectrometry (MS)[4, 5] While this coupling successfully blended the separation power of LC with the sensitivity and selectivity of MS, it created challenges in matching LC flow rate and eluent composition with conditions providing optimal electrospray performance.

The electrohydrodynamic spraying of liquids has been studied since the early 20th century. In 1914 Zeleny's research indicated that an electrospray could be operated in several regimes.[6] Initial classifications included only three regimes – dripping, pulsating, and stable jet – that were readily apparent at increasing applied voltages.[7] Recent classifications[8-12] have grown more complex and confusing, partly due to lack of consensus on nomenclature, and partly due to the scattered experimental observations.

In 1964 Taylor[13] theoretically showed that electrified liquid cones could be stable with semivertical angles of 49.3°. Today such structures are referred to as *Taylor cones* despite the wider range of semivertical angles observed experimentally.[7] Charged liquid is ejected from

Correspondence to: Richard D. Smith.

the cone apex as a jet, which later breaks into small charged droplets due to varicose wave instabilities developed along its surface. This *cone-jet* electrospray regime has proven optimum for many applications and still draws the most scientific attention.

In the *dripping* regime, drops of electrified liquid grow at the tip of a capillary until the combined effect of the gravitational and electrical forces overcomes their surface tension. The drop pinches off and the process, which has been thoroughly described both experimentally and numerically,[14] repeats at relatively low frequency. The drop maintains a rounded profile as long as the gravitational and superficial forces play the major role. At increasing applied voltages, the shape of the ejected liquid (jet or spindle) seems to be affected by its wetting properties.[15]

The *pulsating* regime is manifested at higher voltages and involves liquid ejection at higher frequencies than in the dripping regime. Standing waves on the meniscus surface are responsible for the ejection of liquid jets[16] at a frequency close to that given by Rayleigh's dispersion relation.[17] This relationship[18] predicts the pulsation frequency of a liquid meniscus based on the electrospray emitter (e.g., capillary terminus) radius and liquid physical properties (surface tension and density) and can be used to theoretically divide the dripping and pulsating domains.

The transitions between regimes, induced by changing operating parameters such as voltage or flow rate, can be sudden or chaotic. Chaotic transitions borrow and blend features from the regimes they border and are conspicuous enough to be designated as stand-alone regimes. By increasing the spray voltage of a dripping electrospray, chaotic transitions to the pulsating and then to the cone-jet regimes were observed and recently labeled as *burst*[19] and *astable*[20], respectively. Note, we use the suggested nomenclature[20] to emphasize the difference between spontaneous transitions (e.g., transitions between the pulsating and cone-jet *modes*, as part of the astable *regime*) and transitions induced by a parameter change (e.g., transitions between the pulsating and cone-jet *regimes* due to changes in the applied voltage).

Spray current measurements are useful for diagnosing and deciphering the intricacies of the various electrospray regimes. In early work, Zeleny identified the dripping, burst, pulsating, and cone-jet regimes by running the spray current through a telephone receiver.[6] The current emitted by a cone-jet electrospray has received the most intense theoretical and experimental scrutiny. Inside the stability island of the cone-jet electrospray, a stable Taylor cone forms at the tip of an electrospray emitter for liquids with sufficiently high electric conductivity. The current emitted from a Taylor cone does not depend on the applied voltage (V) and scales with the square root of the surface tension, conductivity, and flow rate of the liquid.[21] In an effort to expand the parameter space, scaling laws have been derived that relate the spray current to the flow rate for polar liquids.[22]

The independence of the spray current from the applied voltage indicates a self-regulating system, which is only partially understood. At least four charge-transfer/transport processes contribute to the successful operation of an electrospray: 1) charge production by electrochemical reaction at the interface between the solution and the electrode where the high voltage is applied, 2) charge migration in the solution toward and along the liquid/gas interface, 3) generation of charged droplets, and 4) movement of charged droplets towards a counter electrode to close the electrical circuit. Van Berkel and coworkers described the cone as a constant current generator whose demand for charge is satisfied by self-regulation of the potential at the electrode/solution interface.[23] Fernández de la Mora and coworkers addressed the self-regulation of the last step by suggesting that the spray adapts itself to transfer to the counter electrode the amount of charge emitted by the cone.[24]

Enke and coworkers attempted to describe the electrospray using electrical circuit theory and implied that the gap between the emitter tip and the counter electrode can be treated as a circuit element characterized by a specific current response to the applied voltage.[25, 26] While e*lectrospray characteristic curves* – plotting the spray current as a function of applied voltage – have been reported,[27-40] they have not been widely nor systematically studied, particularly for the lower flow rates of greatest analytical interest.

The present investigation is part of our efforts to improve the electrospray performance by stabilizing and maintaining it in the cone-jet regime through feedback from spray current measurements. While most commercial mass spectrometers monitor the spray current, this feature is almost never used for active control. Instead, the instrument parameters are usually tuned for the best possible ion current, and visual observation of the Taylor cone provides the comfort of using the electrospray in a regime that resembles the cone-jet. The complex interplay between the spray and ion currents due to charge transfer through the ESI-MS interface[41] implies that electrospray control may be less challenging using spray current rather than ion current measurements. In this study, we emphasize the importance of monitoring the spray current, which can provide valuable information regarding electrospray operation, as well as offer practical benefits associated with analytical stability, sensitivity, and detection limits.

EXPERIMENTAL SECTION

To mimic typical LC-ESI-MS solvent conditions we electrosprayed solutions prepared by mixing the two solvents that we would normally use for gradient elution in our reversed-phase LC systems. Solvent A consisted of 0.2% HOAc + 0.05% TFA in water and solvent B was made with 0.1% TFA in 90:10 acetonitrile:water. The chemicals were purchased from Sigma-Aldrich (St. Louis, MO) and the water was purified by a Barnstead Nanopure Infinity system (Dubuque, IA). Given the typical range for peptide elution, which starts at 5% B and extends up to 60% B, electrospray solutions containing 5%, 15%, 30%, 45%, and 60% B were prepared from batch solvents.

The solutions were delivered by KD Scientific Model 100 syringe pumps through 20-μm-diameter electrospray emitters prepared by chemically etching fused silica capillaries.[42] High voltage generated by a Bertan 205B-03R (Hicksville, NY) power supply was applied to a stainless steel union holding the emitter. Data used to generate electrospray characteristic curves were obtained by measuring the current while scanning the voltage. The spray current was collected by a 50×50 mm stainless steel counter electrode and measured using a LeCroy 9310L 300 MHz oscilloscope (Chestnut Ridge, NY) on its 1 MΩ input impedance. Each current measurement consisted of 500,000 data points acquired at 500 kHz. The distance between the emitter tip and the counter electrode was 2 mm unless otherwise specified. The setup was enclosed in a Faraday cage to minimize the electrical noise. The Taylor cone was observed through a Nikon SMZ1500 stereomicroscope (Tokyo, Japan) equipped with an HR Plan Apo 1x objective lens.

RESULTS AND DISCUSSION

Typical spray current vs. applied voltage characteristic curves are shown in Figure 1 for the 15% B solution. Panel A delineates curve details, while panels B and C focus on general trends. Note that panel A contains error bars for all data points; however, most of the error bars are smaller than the symbols. For clarity, no error bars appear in panels B and C. Chen, et al.[34] presented a characteristic curve similar to the black curve in Figure 1A, which was measured for a flow rate of 30 nL/min. They associated the resistive, low- and high-current self-regulating sections of the curve with the dripping, pulsating, and cone-jet regimes respectively.

In our study, the lack of current oscillations (reflected by the small error bars) precluded the regime identification based solely on current measurements. Using a stereo zoom microscope, visual observation of the electrospray operated at 30 nL/min revealed a curved meniscus with blurred apex at 1200 V and a cone with sharp and well-defined edges at 1400 V. With this supplementary observation, the low- and high-current self-regulating sections of the characteristic curve were confidently associated with the pulsating and cone-jet regimes, respectively. The liquid boundary was the only visual difference between the resistive and the low-current self-regulating sections. At relatively low voltages, the liquid anchored to the outer side of the emitter; the wetted area of the emitter and the volume of liquid at its tip decreased with increasing voltage. Firm anchoring of the liquid to the emitter rim was linked to the transition between the resistive and the low-current self-regulating sections of the characteristic curve. There was no evidence supporting the hypothesis of a dripping electrospray; consequently, the resistive section of the characteristic curve was also associated with the pulsating regime.

The constant current in the cone-jet regime can be explained by the constant generation rate of charged droplets in a stable monodispersed electrospray. The constant current in the pulsating regime is more difficult to understand. A calculation based on Rayleigh's dispersion relation[17] hints at a maximum pulsation frequency of ~122 kHz for water electrosprayed through a 20 μm emitter. This frequency is well within the oscilloscope 500 kHz sampling rate; however, we did not observe current oscillations at this or even at much higher data acquisition rates. At 122 kHz and a 30 nL/min flow rate, volumes of liquid equivalent to droplets of almost 1 μm in radius should be ejected during each pulsation. Droplets of similar size are emitted from larger diameter emitters by electrosprays working in the cone-jet regime.[34] Considering the average current of 66 nA, 5.4×10^{-13} C should be emitted during each pulsation, which is 27 times larger than the Rayleigh limit of a spherical droplet with a 1 μm radius. The liquid is most likely ejected as a whipping jet,[43] which subsequently forms a polydispersed charged aerosol cloud. At the expected spray pulsation frequency, the charged aerosol clouds formed in successive pulses are probably sufficiently overlapped to form a statistically constant spray current.

This justification led us to further investigate the similarities and differences between the pulsating and cone-jet regimes. A current boost at the transition between the two regimes has been observed but remains unexplained. Rayleigh's dispersion relations[18] suggest that the maximum charge density a liquid can hold depends on the smallest length scale of the system. For a pulsating meniscus this length scale should be close to the emitter radius; a larger amount of net charge would destabilize the meniscus, leading to Rayleigh discharges. Recent experimental results seem to confirm that smaller liquid menisci are able to hold larger charge densities.[17] On the other hand, the smallest length scale for a cone-jet geometry should be related to the jet radius; due to its much smaller radius, a jet should be able to hold significantly higher charge densities, and thus sustain larger currents. This hypothesis is in agreement with previous experiments that show liquids with increased conductivities form thinner jets and generate larger spray currents at a given flow rate.[21, 28] It can also explain the combined loss of small amounts of liquid and large amounts of charge during Rayleigh discharges.[44]

In the cone-jet regime the charge is continuously generated electrochemically, and then migrates toward the apex of the Taylor cone before being carried away by droplets that pinch off at the end of the jet. Provided the liquid composition does not change, the potential at the electrode/liquid interface is constant (V_{cj}) and its value ensures that enough charge is generated to sustain the loss through the cone apex.[23]

Evolution of the meniscus in the pulsating regime can be divided into four phases: liquid accumulation, cone formation, liquid ejection, and meniscus recoil.[16] During the liquid

accumulation phase, the meniscus is rounded and the maximum charge density is limited by its curvature. As the liquid becomes increasingly conical, charges start to migrate toward the apex and the smaller curvature allows for increased charge density. The larger amount of charge distorts the field and forces the liquid to adopt a more conical geometry, which results in positive feedback that finally leads to a Rayleigh discharge through a singular point.[45]

Close to the liquid ejection onset the charge distribution and its density along the cone may be similar to those of a cone-jet, but with significant differences in the apex region. Charge is continuously produced electrochemically and accumulates on the liquid surface, inducing its relatively slow geometry change. During the development of the singular point, the geometry of the liquid changes to resemble that of a cone-jet and the existing charge can redistribute towards the cone apex and along the jet. The larger charge requirement boosts the electrode/liquid potential[23] and consequently, the charge production rate. The outcome is dictated by the balance between the charge redistribution rate, characterized by the charge relaxation time, and the charge production rate. If the electrochemistry can supply the increased amount of charge, then the electrospray can switch to the cone-jet regime; otherwise, the charge production rate becomes the limiting factor, leading to discontinuities in charge density. To overcome the limited charge production rate, the potential at the electrode/liquid interface may significantly surpass V_{cj} to allow more species to contribute to the electrochemical process. This could explain the higher degree of analyte oxidation observed for electrosprays in the pulsating regime compared to the cone-jet regime.[43]

At 50 nL/min (red curve in Figure 1A), the characteristic curve shifted to higher voltages and higher currents, and a gradual transition between the two self-regulating regimes was observed. The current measurements in the transitional regime (not shown) resembled those of a continuously charging and discharging RC circuit. The charging curve was similar to that exhibited by the recently described astable regime[20] during the transition from the pulsating to the cone-jet *modes*. The discharge curve of the astable regime was shown to be distorted due to the overlapping current oscillations. In our measurements the lack of current oscillations during the pulsating mode ensured a smooth discharge profile.

The existence of critical (minimum and maximum) flow rates that define a cone-jet stability island is well established.[46] Figure 1B includes characteristic curves measured at flow rates between 20 and 100 nL/min. Since 20 nL/min was defined as the lowest practical flow rate, we did not attempt to completely define the stability island by determining the low critical flow rate. Cone-jet electrospray was established for flow rates between 20 and 80 nL/min, with a notable exception at 70 nL/min. Two important points must be kept in mind when working close to the high critical flow rate: 1) the voltage range inducing a stable cone-jet may be extremely narrow (as in the case of 80 nL/min), and 2) there are random cases when the cone-jet regime cannot be established (as in the case of 70 nL/min).

The transition between the pulsating and cone-jet regimes was sudden at flow rates between 20 and 40 nL/min, and astable at 50, 60, and 80 nL/min. In Figure 1, the astable regime can be readily identified because of the large error bars (1A) and the varying slope of the characteristic curves (1B and 1C). Generally, if the astable regime was not present in the characteristic curve at a given flow rate, it was not present at lower flow rates. Similarly, if the astable regime was present in a characteristic curve at a given flow rate, then it was also present at higher flow rates. Even at flow rates outside the cone-jet stability island, the regime sequence included the astable regime. For example, at 100 nL/min (blue curve in Figure 1A), the spray was astable between 1400 and 1530 V, but did not reach the cone-jet regime at increased voltages. At 200 nL/min (green curve in Figure 1A) the presence of the astable regime was minimal.

For all practical purposes, the characteristic curves at larger flow rates resembled the curve at 200 nL/min, with no astable transition. The formation of liquid drops on the counter electrode was another common occurrence at relatively large flow rates. For example, when electrospraying the 5% B solution, drop formation on the counter electrode was noticed at flow rates as low as 100 nL/min. With increasing flow rates, a stream of small droplets that sustained a faster drop growth on the counter electrode became progressively more visible.

These observations have important implications for ESI-MS analyses. For liquids typically used as electrospray solvents, a visible droplet stream ejected from a Taylor cone indicates that the electric field does not efficiently disperse the liquid because of a large flow rate or a low applied voltage. Increasing the voltage may help only if the flow rate is between the critical flow rates that define the cone-jet stability island. We refer to the regime in which the electrospray works at a flow rate larger than critical as *jetting*. In this regime, the amount of charge is not large enough to efficiently disperse the jet emerging from the Taylor cone. Thus, some of the analyte molecules can not form gas-phase ions, leading to biased detection effects and degraded sensitivity.

Even in the jetting regime, the electrospray may efficiently produce a good quality charged aerosol. In fact, commercial mass spectrometer designs often address the problem of a large flow rate by avoiding the central stream of larger droplets and sampling the periphery of the spray that is enriched by very much smaller progeny droplets originating both from the initial jet breakup process and from Rayleigh discharges of larger parent droplets.[47] Heating the mass spectrometer inlet leads to rapid liquid evaporation, which in turn hides the drop accumulation and growth on the interface. From here onwards, we focus our discussion solely on results obtained at flow rates inside the cone-jet stability island and note that the conclusions may not be valid for the jetting regime.

The characteristic curves measured at flow rates between 20 and 80 nL/min for 5% B solution are plotted in Figure 1C. The experimental points measured at relatively large voltages appear to sit on a line, which we will refer to as the *cone-jet breakdown line*. The area at the right of the breakdown line will be called the *cone-jet breakdown region*. The gap between the emitter and the counter electrode can be characterized by a resistance of 3.94 GΩ, which includes the resistance of the column of liquid inside the emitter.[25] The breakdown line intersects the abscissa at an applied voltage of 1.27 kV. This voltage, part of which drops on the column of liquid inside the emitter, is too small to induce air breakdown between parallel plates; however, because of the large electric field at the tip in a tip-to-plane geometry,[48] air breakdown is possible at smaller applied voltages.

With increased voltage, the data points in Figure 1C seem to approach the breakdown line at relatively constant current and then follow it. At the intersection between the two lines the mechanism of charge production and/or charge transport clearly changes. Although this work provides no evidence to either support or reject the hypothesis of an electrical breakdown or a corona discharge, we suggest that the measured spray current may be partly due to ionized gas molecules. A second breakdown increases the current even more; this effect is visible in Figure 1A and Figure 1C (red curves). We attribute this behavior to small scale imperfections of the emitter that may act as discharge points that ionize the surrounding gas and boost the total measured current. The second breakdown is avoided at larger flow rates due to improved coverage of the emitter afforded by the liquid.

At 20 nL/min (red curve in Figure 1C) the data show one type of major exception, whereby the electrospray collapses to the breakdown line before the two lines theoretically meet. We occasionally observed this behavior with different solutions and/or at higher flow rates (data not shown), and suspect that outer emitter wetting is responsible for this effect. Another type

of exception that occurs more frequently is evident in Figure 1A. In this case, the characteristic curve penetrates into the breakdown region before the current jumps to follow the breakdown line. We estimated a resistance of 1.95 GΩ and a breakdown voltage of 1.13 kV from the linear fitting coefficients of this breakdown line (not shown). Since measurements were performed with different solutions that were electrosprayed through different emitters, we expected a different resistance value. The breakdown voltage is within 15% of the previous calculated value; the difference may be related to differences in sprayed solution, emitter length, and distance to the counter electrode.

An increase in the distance between the emitter and the counter electrode might be expected to decrease the field strength at the emitter tip and shift the regime onset voltages to larger values. The electrospray characteristic curves (Figure 2A) show that the distance has minimal effect on the magnitude of the current emitted in the cone-jet regime. One of the obvious effects was the decrease of the breakdown current with increasing distance to the counter electrode.

The less obvious effects are captured by the regimes map in Figure 2B. The logarithmic dependence of the electric field at the emitter tip as a function of the distance to the planar counter electrode[48] can explain the relatively minor shift of the onset voltages that occurs with relatively large changes of the distance to counter electrode. Unexpectedly, the onset voltage goes through a minimum at a distance (3 mm in Figure 2B) that we will refer to as the *optimum distance*. Coincidentally, the transition is sudden at distances smaller than the optimum distance (2 and 2.5 mm) and astable at distances larger than or equal to the optimum distance, although this observation does not always hold. However, if the astable regime is present in a characteristic curve at a given distance, then it is very likely that this regime would also be present at larger distances. Similarly, if the astable transition is not present in the characteristic curve at a given distance, most likely this transition would not be present at smaller distances either. This observation could be extrapolated to the characteristic curves in Figure 1B. It is possible that decreasing the distance to counter electrode would lead to a sudden rather than astable transition for a flow rate of 50 nL/min, while increasing the distance may induce an astable transition in the characteristic curve at 40 nL/min.

Reproducibility of these curves was generally good. Shifts of 10–20 V in the onset voltages were not unusual; however, results obtained with the same emitter compared well. Similar trends were obtained using different emitters, in spite of larger shifts in the onset voltages and/or spray current values. Expectedly, decreasing the applied voltage induced a spray current hysteresis at the transition between the cone-jet and the pulsating regimes, manifested by a collapse to the pulsating regime at a voltage (V_p) 30-50 V lower than the voltage corresponding to the onset of the cone-jet regime (V_o).

Fernández de la Mora brought theoretical support to the existence of electrospray hysteresis phenomenon by showing that the mathematical solution to the shape of the cone for an electrospray operating in the cone-jet regime at a given voltage is not unique.[49] We further suggest that liquid dynamics can account for the hysteresis at the boundary between the pulsating and the cone-jet domains. In the pulsating regime, standing waves on the liquid meniscus are responsible for periodic liquid ejection followed by powerful recoils.[16] The recoils nourish the wave energy, which keeps the meniscus in pulsating motion even when the voltage reaches values larger than V_p, at which the electrospray may be stable in the cone-jet regime. In the cone-jet regime the liquid is stationary, so the wave leading to meniscus pulsation must be initiated by a fluctuation in charge production/migration or by a mechanical event. This requirement can explain the electrospray tendency to remain in the cone-jet regime for voltages lower than V_o.

Figure 3 compares regime maps measured for solutions of 5%, 30%, 45% and 60% solvent B electrosprayed through the same emitter. These maps could be used to optimize the ion source operation during an RPLC-ESI-MS analysis. For example, at a flow rate of 20 nL/min, a voltage set around 1.3 kV would ensure electrospray operation in the cone-jet regime; however, by the end of the analysis the optimum voltage would shift down by almost 200 V. Manual voltage control may be feasible for continually monitored experiments, but is generally impractical.

Programming a voltage change based on the eluent concentration is one possible solution. However, this approach would not account for the use of different emitters, the same emitter positioned differently, or effects due to changes in the emitter that occur e.g. as insoluble or microscopic residue accumulates on internal or external surfaces of the emitter. Numerous other factors such as temperature, instrumental drift, etc. may also contribute to the failure of such an approach. Changes in the liquid properties during analyte elution may also induce changes in the electrospray regime. All of these factors point to the need for active control of the electrospray operation. The literature reports a single attempt to automatically maintain the electrospray in the cone-jet regime by adjusting the voltage based on feedback from spray imaging.[50] Using spray current measurements for feedback may provide an alternative solution, which could be more attractive in terms of cost and simplicity.

In addition to the changes in the onset voltages, another trend is apparent in Figure 3B: the astable regime penetrates to lower flow rates with increasing concentration of solvent B. This effect further complicates the design of the spray-control system. That is, actively changing the distance to the counter electrode would greatly complicate the setup and drive up the cost; however, this change may compensate for the astable regime and provide improved control over the desolvation process.[41]

CONCLUSIONS

There are many benefits to operating the electrospray in the cone jet regime, and these benefits persist in the nanoelectrospray flow regime of high analytical interest. Depending on the analyte, the ion current can increase by a factor of 2 to 10 when the electrospray switches from the pulsating to the cone-jet regime.[43] However, maintaining the electrospray in the cone-jet regime can be difficult, especially during liquid separations. In this study, we mimicked the solvent composition of a gradient separation and varied electrospray flow rate and the distance between the emitter and the counter electrode to generate electrospray characteristic curves. In this context, we revealed some of the factors that induce an astable transition in electrospray. Further experiments on liquids with well-controlled physical properties are necessary to understand the phenomena more quantitatively.

Without active control of the electrospray, major ion signal fluctuations are to be expected as the spray moves in and out of its cone-jet stability island. The working regime of low-flow electrosprays can be altered by changes in solution composition and other minor changes (e.g. to the emitter). Operating the electrospray at larger flow rates on the breakdown line can be a good compromise, in spite of fractionation effects and degraded sensitivity.

We have shown that spray current measurements provide a potentially reliable feedback mechanism for automatically maintaining an electrospray inside its cone-jet stability island. This approach is also feasible at very low flow rates where optical approaches may become less practical. A system that ensures electrospray operation in the cone-jet regime would allow reliable operation at low flow rates, even with complex solvent mixtures such as those eluting from an HPLC. Lower flow rates would provide increased sensitivity and detection limits, while the added stability would be beneficial for most quantitative applications.

Acknowledgements

The Pacific Northwest National Laboratory (PNNL) machine shop and Dr. Anil Shukla are acknowledged for their help in building the Faraday cage. We gratefully acknowledge the contributions of Penny Colton in preparing this publication. This research was supported by the NIH National Center for Research Resources (RR018522). Experimental portions of this research were performed in the Environmental Molecular Sciences Laboratory, a DOE national scientific user facility located at the PNNL in Richland, Washington. PNNL is a multiprogram national laboratory operated by Battelle for the DOE under Contract DE-AC05-76RLO 1830.

References

1. Tanaka K, Waki H, Ido Y, Akita S, Yoshida Y, Yoshida T, Matsuo T. Rapid Communications in Mass Spectrometry 1988;2:151–153.
2. Karas M, Hillenkamp F. Analytical Chemistry 1988;60:2299–2301. [PubMed: 3239801]
3. Mann M, Meng CK, Fenn JB. Analytical Chemistry 1989;61:1702–1708.
4. Aleksandrov ML, Gall LN, Krasnov VN, N VI, Pavlenko VA, Shkurov VA, Baram GI, Gracher MA, Knorre VD, Kusner YS. Bioorg Khim 1984;10:710–712.
5. Whitehouse CM, Dreyer RN, Yamashita M, Fenn JB. Analytical Chemistry 1985;57:675–679. [PubMed: 2581476]
6. Zeleny J. Physical Review 1914;3:69–91.
7. Hayati I, Bailey AI, Tadros TF. Journal of Colloid and Interface Science 1987;117:205–221.
8. Cloupeau M, Prunetfoch B. Journal of Aerosol Science 1994;25:1021–1036.
9. Grace JM, Marijnissen JCM. Journal of Aerosol Science 1994;25:1005–1019.
10. Shiryaeva SO, Grigorev AI. Journal of Electrostatics 1995;34:51–59.
11. Juraschek R, Rollgen FW. International Journal of Mass Spectrometry 1998;177:1–15.
12. Jaworek A, Krupa A. Journal of Aerosol Science 1999;30:873–893.
13. Taylor G. Proceedings of the Royal Society of London Series A-Mathematical and Physical Sciences 1964;280:383–397.
14. Zhang XG, Basaran OA. Journal of Fluid Mechanics 1996;326:239–263.
15. Reznik SN, Yarin AL, Theron A, Zussman E. Journal of Fluid Mechanics 2004;516:349–377.
16. Marginean I, Parvin L, Heffernan L, Vertes A. Analytical Chemistry 2004;76:4202–4207. [PubMed: 15253664]
17. Marginean I, Nemes P, Parvin L, Vertes A. Applied Physics Letters 2006;89:064104.
18. Rayleigh L. Philosophical Magazine 1882;14:184–186.
19. Marginean I, Nemes P, Vertes A. Physical Review Letters 2006;97:064502. [PubMed: 17026172]
20. Marginean I, Nemes P, Vertes A. Physical Review E. 2007accepted
21. Fernández de la Mora J, Loscertales IG. Journal of Fluid Mechanics 1994;260:155–184.
22. Gañán-Calvo AM. Journal of Fluid Mechanics 2004;507:203–212.
23. Van Berkel GJ, Zhou FM. Analytical Chemistry 1995;67:2916–2923.
24. Aguirre de Carcer I, Fernández de la Mora J. Journal of Colloid and Interface Science 1995;171:512–517.
25. Jackson GS, Enke CG. Analytical Chemistry 1999;71:3777–3784. [PubMed: 10489527]
26. Cech NB, Enke CG. Mass Spectrometry Reviews 2001;20:362–387. [PubMed: 11997944]
27. English WN. Physical Review 1948;74:179–189.
28. Smith DPH. IEEE Transactions on Industry Applications 1986;22:527–535.
29. Ikonomou MG, Blades AT, Kebarle P. Analytical Chemistry 1991;63:1989–1998.
30. Ikonomou MG, Blades AT, Kebarle P. Journal of the American Society for Mass Spectrometry 1991;2:497–505.
31. Meesters GMH, Vercoulen PHW, Marijnissen JCM, Scarlett B. Journal of Aerosol Science 1991;22:S11–S14.
32. Meesters GMH, Vercoulen PHW, Marijnissen JCM, Scarlett B. Journal of Aerosol Science 1992;23:37–49.

33. Kriger MS, Cook KD, Ramsey RS. Analytical Chemistry 1995;67:385–389. [PubMed: 7856882]
34. Chen DR, Pui DYH, Kaufman SL. Journal of Aerosol Science 1995;26:963–977.
35. Borra JP, Tombette Y, Ehouarn P. Journal of Aerosol Science 1999;30:913–925.
36. Constantopoulos TL, Jackson GS, Enke CG. Analytica Chimica Acta 2000;406:37–52.
37. López-Herrera JM, Barrero A, Boucard A, Loscertales IG, Márquez M. Journal of the American Society for Mass Spectrometry 2004;15:253–259. [PubMed: 14766292]
38. Parvin L, Galicia MC, Gauntt JM, Carney LM, Nguyen AB, Park E, Heffernan L, Vertes A. Analytical Chemistry 2005;77:3908–3915. [PubMed: 15987091]
39. Alexander MS, Paine MD, Stark JPW. Analytical Chemistry 2006;78:2658–2664. [PubMed: 16615777]
40. Paine MD, Alexander MS, Stark JPW. Journal of Colloid and Interface Science 2007;305:111–123. [PubMed: 17028003]
41. Page JS, Kelly RT, Tang K, Smith RD. Journal of the American Society for Mass Spectrometry. 2007in press
42. Kelly RT, Page JS, Luo QZ, Moore RJ, Orton DJ, Tang KQ, Smith RD. Analytical Chemistry 2006;78:7796–7801. [PubMed: 17105173]
43. Nemes P, Marginean I, Vertes A. Analytical Chemistry 2007;79:3105–3116. [PubMed: 17378541]
44. Li KY, Tu HH, Ray AK. Langmuir 2005;21:3786–3794. [PubMed: 15835938]
45. Oddershede L, Nagel SR. Physical Review Letters 2000;85:1234–1237. [PubMed: 10991520]
46. Cloupeau M, Prunetfoch B. Journal of Electrostatics 1989;22:135–159.
47. Tang KQ, Smith RD. Journal of the American Society for Mass Spectrometry 2001;12:343–347. [PubMed: 11281610]
48. Eyring CF, Mackeown SS, Millikan RA. Physical Review 1928;31:900–909.
49. Fernández de la Mora J. Annual Review of Fluid Mechanics 2007;39:217–243.
50. Valaskovic GA, Murphy JP, Lee MS. Journal of the American Society for Mass Spectrometry 2004;15:1201–1215. [PubMed: 15276167]

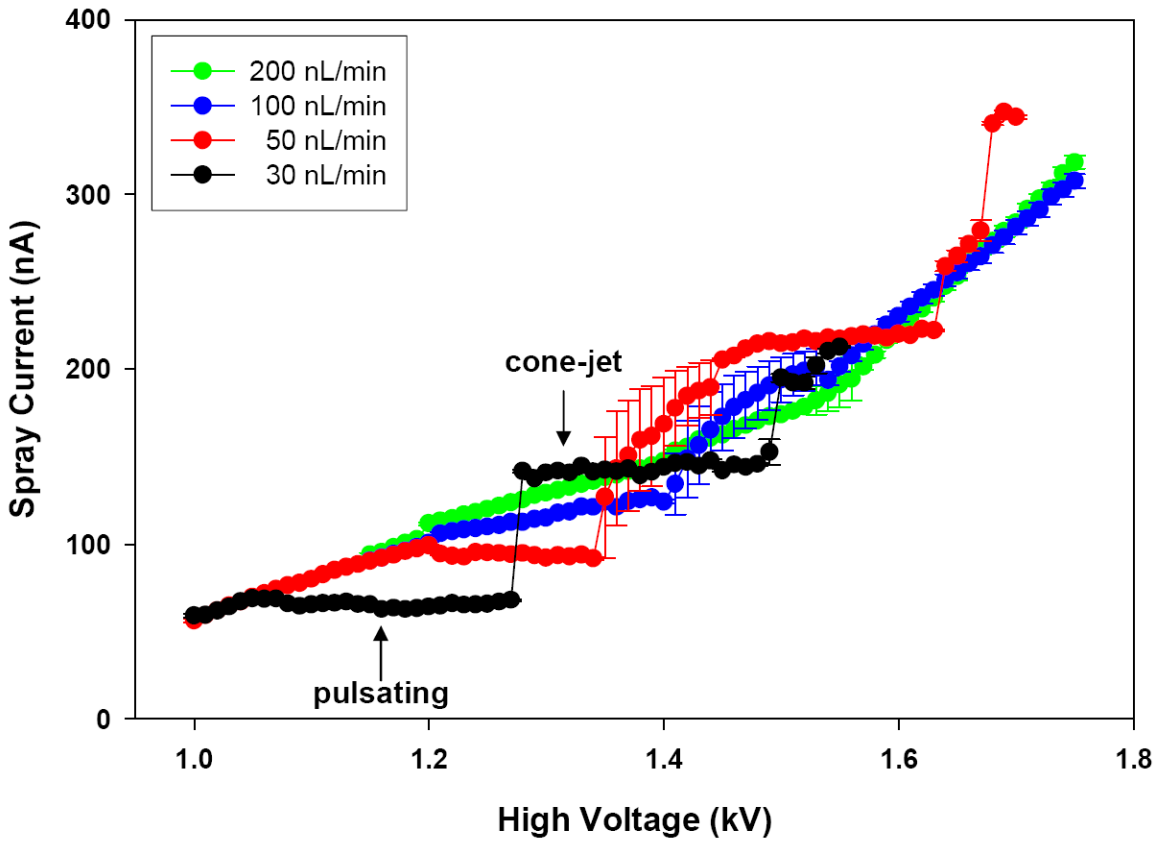

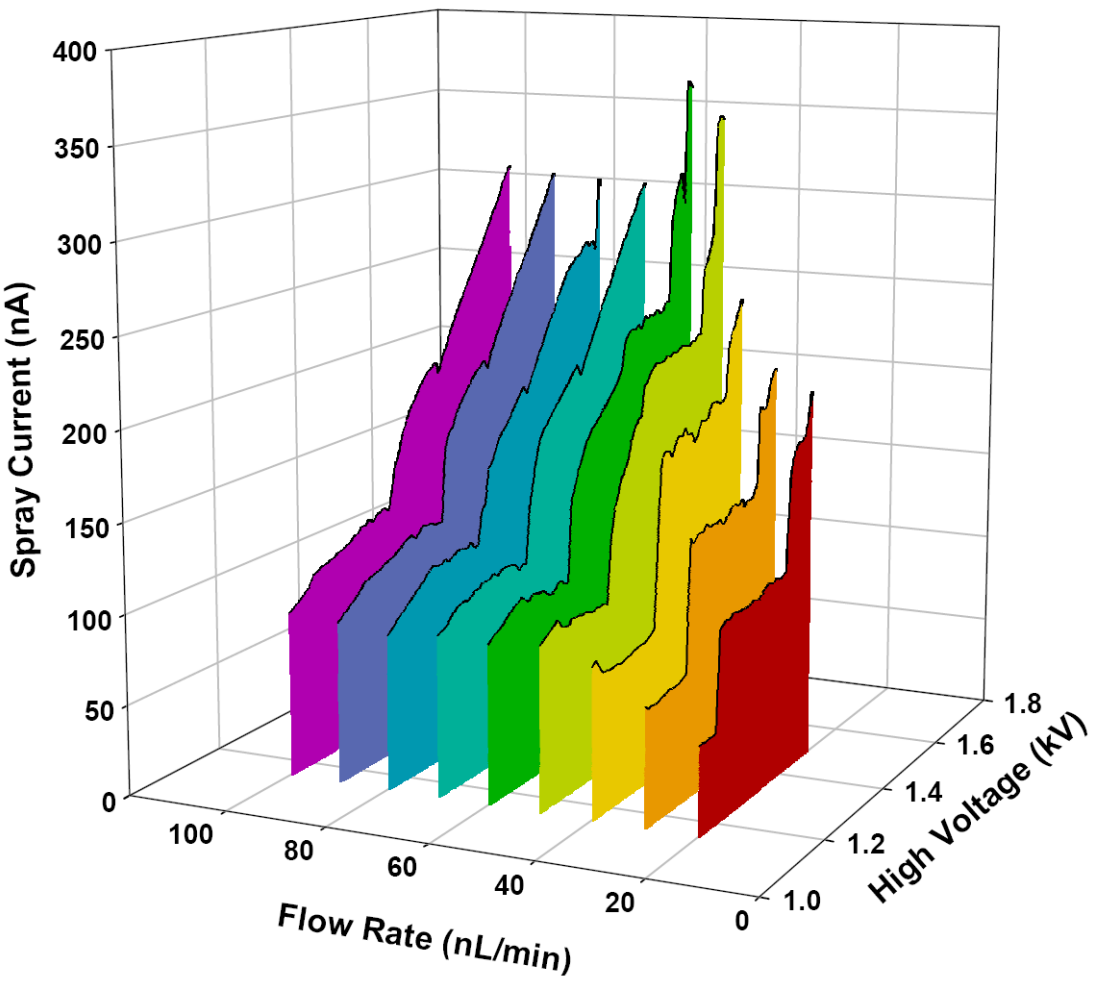

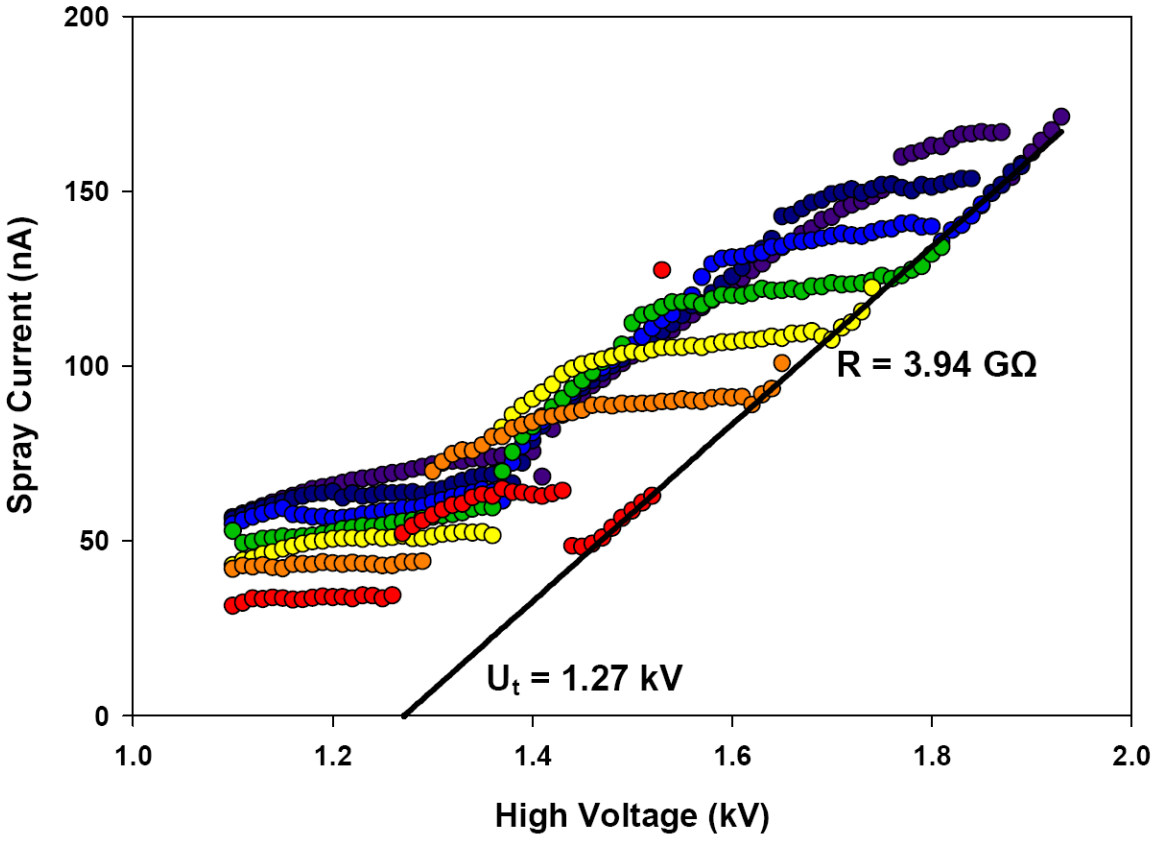

Figure 1.
Characteristic curves measured for 15% B solution at 30, 50, 100 and 200 nL/min reflect the regime sequence an electrospray undergoes with increasing applied voltage (A). General trends for flow rates between 20 and 100 nL/min, partially illustrating the cone-jet stability island (B). General trends indicating the breakdown line and the breakdown region (C).

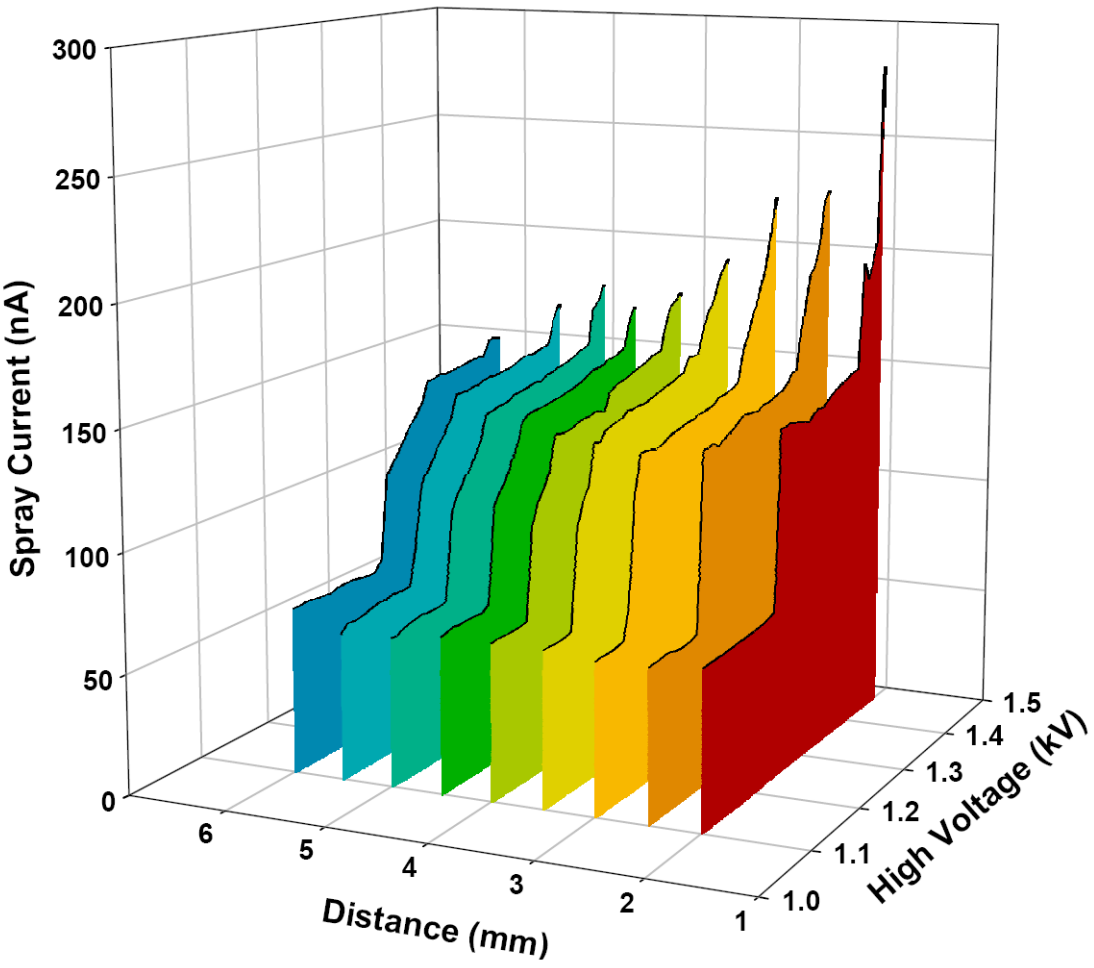

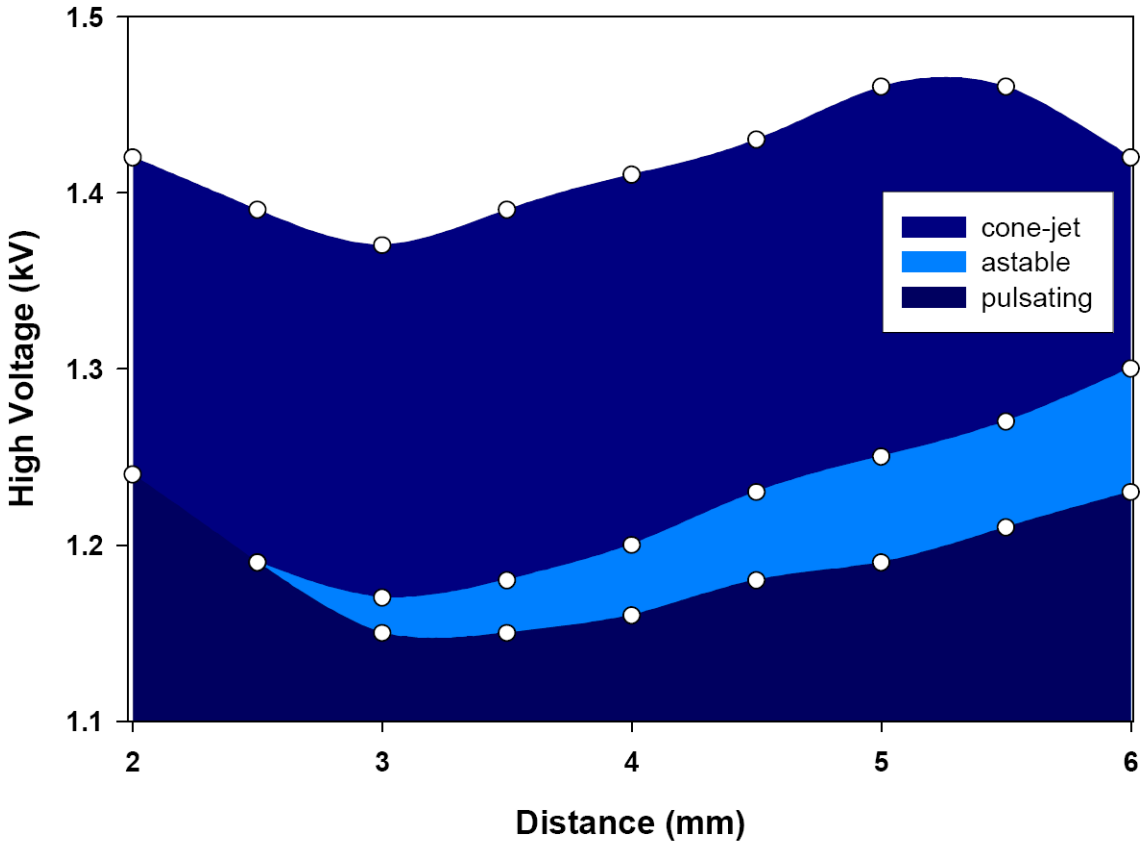

Figure 2.
Effect of emitter-to-counter-electrode distance on characteristic curves measured for 15% B solution at 20 nL/min (A) and corresponding regime map (B).

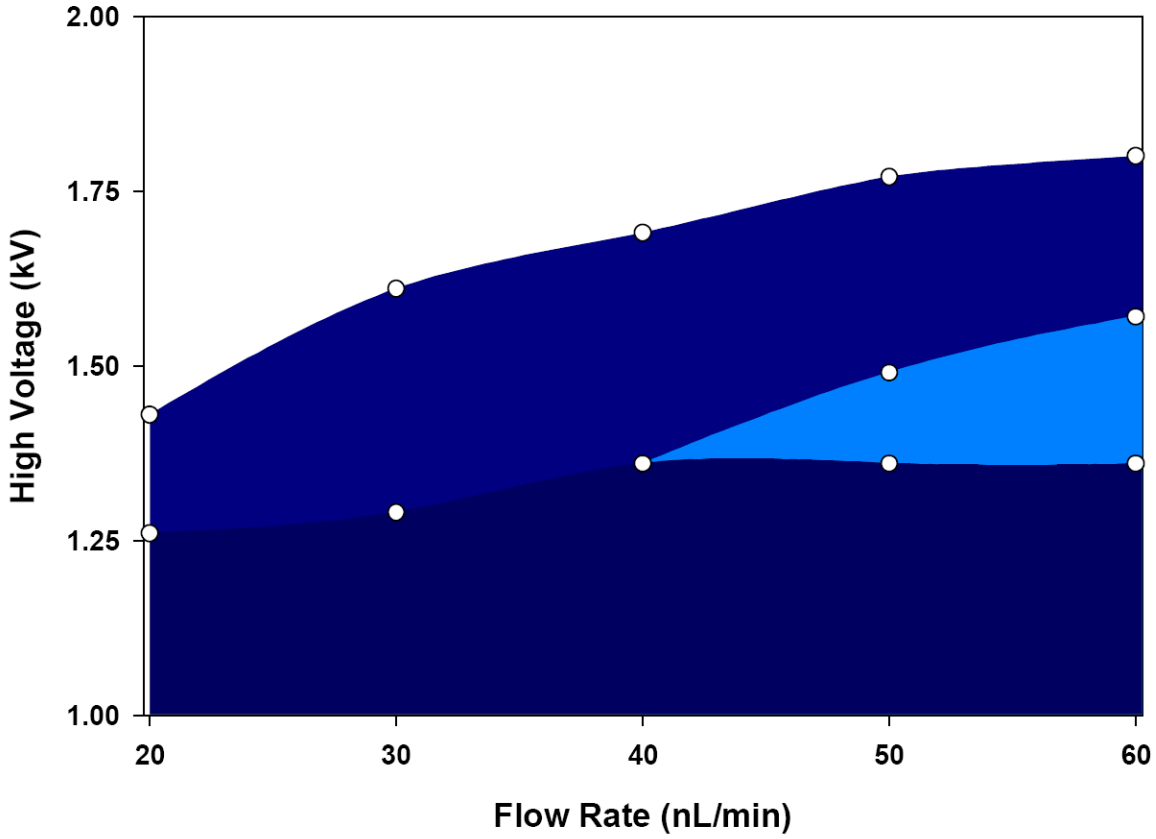

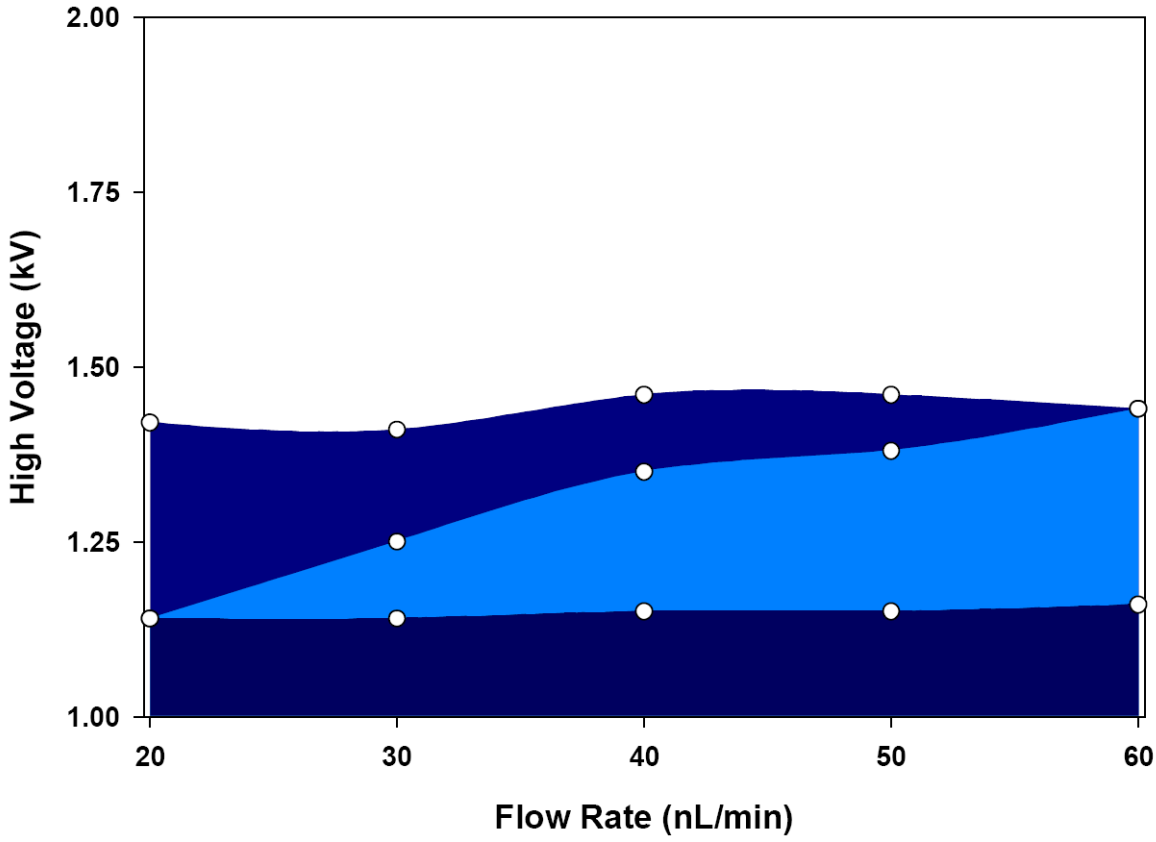

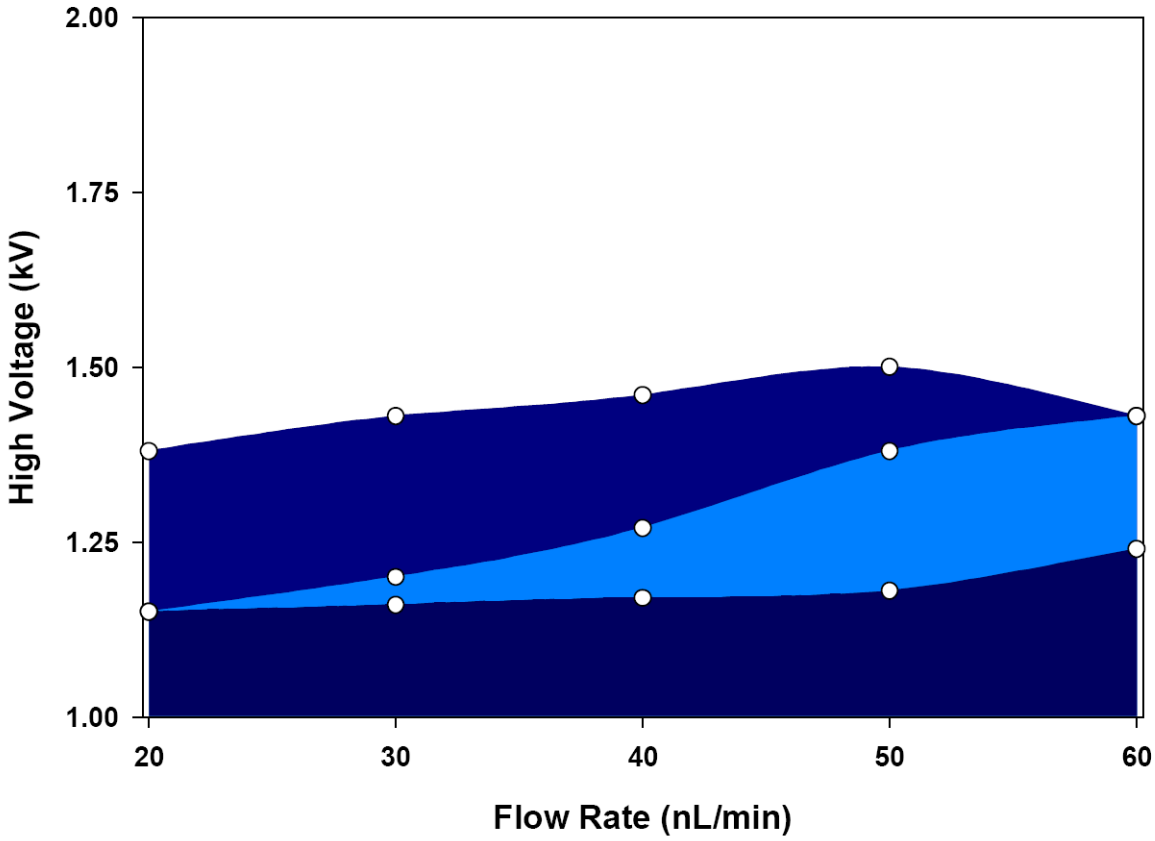

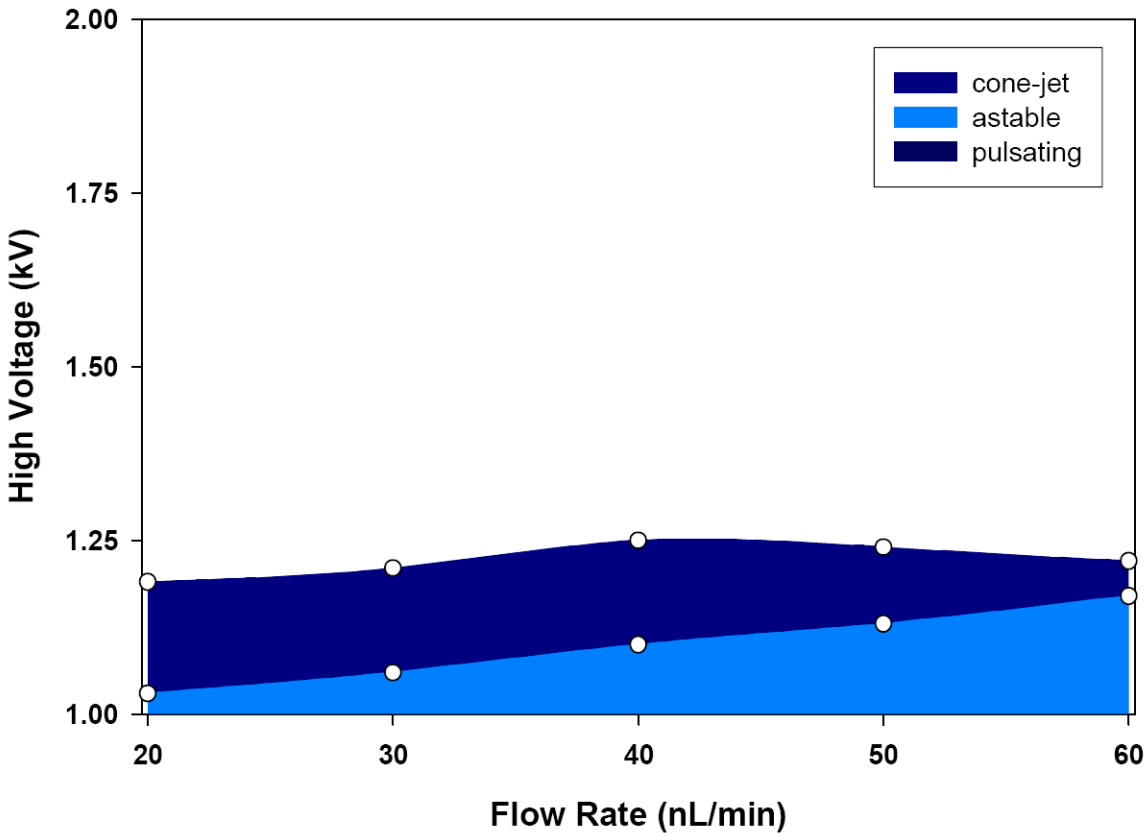

Figure 3.
Regime maps for several concentrations of solvent B: 5% (A), 30% (B), 45% (C) and 60% (D) (see Experimental).